Journal of Computer-Aided Molecular Design, 8 (1994) 709–730
ESCOM

J-CAMD 269

Pharmacophore refinement of gpIIb/IIIa antagonists based on comparative studies of antiadhesive cyclic and acyclic RGD peptides

Gerhard Müller*, Marion Gurrath** and Horst Kessler***

Institut für Organische Chemie und Biochemie, Technische Universität München, Lichtenbergstrasse 4, D-85747 Garching, Germany

Received 7 April 1994
Accepted 6 July 1994

Key words: Arg-Gly-Asp peptides; Adhesion antagonists; Peptide templates; Conformational restriction; Vector analysis; Structure–activity relationships

SUMMARY

Structurally guided design approaches to low-molecular-weight platelet aggregation antagonists addressing the platelet-associated heterodimeric cell surface receptor gpIIb/IIIa rely on comparative studies of an ensemble of conformationally and biologically characterized compounds, since no high-resolution structure of the receptor system is available. We report a classical indirect and comparative pharmacophore refinement approach based on a series of small cyclic Arg-Gly-Asp (RGD) peptides as gpIIb/IIIa–fibrinogen interaction antagonists. These peptides have previously been investigated as potent and selective tumor cell adhesion inhibitors. The definition of geometrical descriptors classifying the RGD peptide conformations and their subsequent analysis over selected RGD- and RXD-containing protein structures allows for a correlation of distinct structural features for platelet aggregation inhibition. An almost parallel alignment of the Arg and Asp side chains was identified by a vector analysis as being present in all active cyclic hexa- and pentapeptides. This orientation is induced mainly by the constraint of backbone cyclization and is not of any covalent tripeptide-inherent origin, which was rationalized by a 500 ps high-energy MD simulation of a sequentially related linear model peptide. The incorporation of the recognition tripeptide Arg-Gly-Asp into the cyclic peptide templates acted as a filter mechanism, restricting the otherwise free torsional relation of both side chains to a parallel orientation. Based on the derived results, several detailed features of the receptor binding site could be deduced in terms of receptor complementarity. These findings should govern the design of next-generation compounds with enhanced activities. Furthermore, the complementary stereochemical characteristics of the substrate can be used as boundary conditions for pseudoreceptor modelling studies that are capable of reconstructing a hypothetical binding pocket, qualitatively resembling the steric and electronic demands of gpIIb/IIIa. It is interesting to note that these features provide clear differentiation to requirements for inhibition of $\alpha_v\beta_3$ substrate binding. This can account for the extremely high selectivity and activity of some of our constrained peptides for either the $\alpha_{IIb}\beta_3$ or the $\alpha_v\beta_3$ receptor.

*Present address: Bayer AG, MD-IM-FA, Computational chemistry, Gebäude Q18, D-51368 Leverkusen, Germany.
**Present address: University of Padua, Biopolymer Research Centre, Department of Organic Chemistry, Via Marzolo 1, I-35131 Padua, Italy.
***To whom correspondence should be addressed.

INTRODUCTION

One of the fundamental aims of rational drug design is to gain insights into molecular processes that govern the binding of small molecules to more complex macromolecular systems, i.e., the target receptor [1,2]. If three-dimensional (3D) structural information of a receptor–substrate complex, or at least of the receptor alone is available, an understanding of how a ligand interacts with the subsite of its receptor by different specific contacts can be rationalized on an atomic level (see for example Refs. 3–7). However, most receptor systems that are targeted by drugs of current pharmaceutical interest are membrane-bound multidomain proteins, the 3D structures of which are unknown at present [2]. Therefore, the molecular site of action of active compounds in a relevant biological assay is unknown and has to be established via an indirect design and optimization procedure based on a series of biologically and structurally characterized compounds [8–10].

We utilized this indirect strategy for the design of synthetic cyclic oligopeptides with preferred backbone conformations [11]. Conformationally constrained peptides of this kind can be promising tools for scanning the physicochemical and steric requirements of a receptor under study and can provide new lead structure information in terms of pharmacophore functionalities and geometries [12,13]. We have recently described a conformationally guided design strategy of a series of cyclic Arg-Gly-Asp-containing peptides (commonly termed RGD peptides), together with their chemical synthesis, conformational analysis and the study of conformation–activity relationships. Some of these RGD peptides modulate tumor cell adhesion in a highly active and selective manner [14].

The primary biochemical target of Arg-Gly-Asp-containing peptides in pharmaceutical research so far has been the inhibition of platelet aggregation by binding to the platelet cell surface receptor gpIIb/IIIa ($\alpha_{IIb}\beta_3$) in competition with the native substrates, principally fibrinogen and Von Willebrand factor [15–18]. The glycoprotein gpIIb/IIIa is a member of the integrin superfamily of cell surface receptors that mediate a variety of adhesive processes in organisms on a cellular level, including the pathogenic processes of tumor metastasis, osteoporosis and blood clot formation [19–24]. It is well documented in the literature that the universal recognition sequence Arg-Gly-Asp, whether incorporated into synthetic peptides [25–36], peptidomimetics [37–40] or in a number of isolated snake venoms [41–48], determines the affinity and specificity of numerous adhesive protein–integrin interactions. Therefore, RGD-derived compounds have been extensively discussed as potential antithrombotic or antimetastatic agents. Since no 3D structure at atomic resolution of the gpIIb/IIIa receptor is available at present, all structure–activity studies are based on comparative investigations of platelet aggregation antagonists.

In this paper we describe the high biological activities of the previously designed tumor cell adhesion antagonists [14,34] to isolated $\alpha_{IIb}\beta_3$ [49]. We further propose a working hypothesis regarding the steric demand of the receptor binding pocket by comparison of NMR-derived and MD (molecular dynamics)-refined conformations of a series of cyclic RGD peptides with their inherent binding capabilities to gpIIb/IIIa. The cyclic penta- and hexapeptides used for this study have the distinct advantage that they are among the smallest highly potent peptides. They have strongly reduced backbone mobility and have been conformationally characterized by experimental NMR data and restrained MD calculations [14]. The selection of a set of geometrical descriptors for structure–activity relationships that allow for a correlation of conformational parameters

with receptor binding data is presented. These descriptors account for the relative alignment of the arginine and aspartic acid side chains, based on a vector analysis closely related to the philosophy of the 3D search program CAVEAT (computer-assisted vector evaluation and target design), developed by Bartlett et al. [50]. The result of the vector analysis applied to the RGD peptide conformations will be compared with X-ray structures of selected Arg-Xaa-Asp-containing proteins from the Brookhaven Protein Data Bank (PDB), with NMR-derived conformations of the Arg-Gly-Asp-containing snake venoms kistrin [51] and echistatin [52–54] and with the results of an MD simulation of the model peptide Ac-Gly-Arg-Gly-Asp-Phe-Gly-$NHCH_3$, in order to explore the available conformational space for the defined structural descriptors.

The sensitivity of the essential tripeptide sequence Arg-Gly-Asp to stereochemical modifications, as well as to additional CH_3 substitutions, will be highlighted and the results will be compared to studies of the same peptides directed against vitronectin and laminin fragment P1 receptors [14,34]. This information should provide novel insight into the discriminating behaviour of receptor subtypes of the same receptor superfamily.

MATERIALS AND METHODS

Cyclic RGD peptides and proteins

The design of cyclic penta- and hexapeptides discussed in this investigation follows a strategy that is based on the use of two common structural templates by introduction of a D-amino acid into the primary sequence. The details of the design, the chemical synthesis and the conformational analysis by means of 2D NMR spectroscopy and restrained MD simulations for structure refinement are given in Ref. 14.

The protein structures containing an Arg-Xaa-Asp sequence are taken from the Brookhaven PDB; the coordinates of kistrin [51] and echistatin [52] have kindly been provided by G. Wagner and J. Pelton, respectively.

Molecular dynamics simulations

The molecular dynamics simulation of the model compound Ac-Gly-Arg-Gly-Asp-Phe-Gly-$NHCH_3$ was carried out over 500 ps at a temperature of 1000 K. For this simulation and for all graphical analyses and interactive animations the Biosym molecular modelling software was used (available from Biosym Technologies Inc., San Diego, CA). The MD simulation was carried out within the consistent valence force field (cvff), without Morse potentials for bond stretching interactions and without cross terms [55]. For numerical integration of the equation of motion the Verlet algorithm [56] was used, with a time step of 1 fs. The linear peptide was initialized to a temperature of 1000 K over 10 ps; subsequently, 500 ps were simulated. The trajectory was updated every 0.25 ps in order to store 2000 frames of the dynamics. The starting structure was modelled interactively; the amino acid residues were taken from the INSIGHT residue library. The Arg-Gly-Asp sequence was flanked by residues at the C- and N-termini to avoid conformational distortions during the simulation due to terminal charge effects. Additionally, the N-terminal and C-terminal glycines were blocked by an acetyl and an *N*-methylamide group, respectively, in order to mimic the adjacent peptide chain. All peptide bonds were modelled in trans configuration, and all ϕ and ψ backbone dihedrals adopted the 180° conformation. The unusually long simulation period of 0.5 ns and the rather high temperature of 1000 K were chosen in order

to ensure that the molecule is able to effectively sample the conformational space in the course of the simulation.

The simulations were carried out on a Silicon Graphics 4D/240SX computer and the graphical animations were done using a Silicon Graphics 4D/Crimson, equipped with an Elan Graphics terminal.

Biological assays

Solid-phase binding assays have been carried out in order to examine the inhibitory potentials of the discussed oligopeptides. Two alternative strategies were followed, i.e., either the $\alpha_{IIb}\beta_3$ integrin or the protein ligand were immobilized. In the first case the soluble protein ligand was mixed with the peptide and incubated at room temperature in coated wells containing the receptor. An ELISA (enzyme-linked immunosorbant assay)-type assay allowed detection of ligand binding by using anti-ligand antibodies as primary antibody. In the second variant the protein ligand was immobilized and soluble integrin was preincubated with the peptide before addition to the protein ligand-coated wells. The activities were then expressed as IC_{50} values (inhibitory capacity, molar concentration for 50% inhibition) derived from typical peptide concentration-dependent inhibition profiles. All assays have been carried out repeatedly in order to minimize artifacts and to define the statistical significance of these IC_{50} values.

The $\alpha_{IIb}\beta_3$ integrin was purified chromatographically from detergent extracts of human platelets and characterized by SDS (sodium dodecylsulfate) gel electrophoresis, followed by protein staining or immunoblotting. A more detailed discussion of the experimental procedure, especially addressing the quantitative difference of the derived IC_{50} values from the above described solid-phase assays, is given in Refs. 49 and 57.

RESULTS

Biological activities

The inhibitory activities of all tested cyclic RGD peptides are given in Table 1 according to the numbering scheme introduced previously [14]. The linear peptide GRGDS was used as reference compound. It is remarkable that some of the peptides demonstrated inhibitory activities comparable to soluble fibrinogen, which is the native substrate of gpIIb/IIIa. The solid-phase assays carried out with either soluble (assay A) or plastic-immobilized (assay B) integrins reveal large differences in IC_{50} values, depending on the experimental set-up (Table 1). In general, the IC_{50} values of assay B are increased by a factor of 100–200 when compared to assay A, which was carried out with soluble integrin. Since most investigations published in the literature rely on solid-phase inhibition assays, we use these IC_{50} values for our comparative discussion regarding structure–activity studies. Nevertheless, we have shown recently that calibrating the inhibition constants by applying the physical method of total internal reflection fluorescence microscopy (TIRFM), followed by normalization, yielded relative binding activities of the peptides which are less affected by the different assay conditions [49].

The D-Phe-containing cyclic hexapeptides show the highest activities, with IC_{50} values of 0.03–0.17 and about 10 μM in assays A and B, respectively. Among these compounds the peptides **11** and **12**, with glycine in position 6, i.e., the residue preceding the essential tripeptide sequence, demonstrate moderately higher inhibition when compared to the alanine-containing

homologues **9** and **10**. In this subfamily of peptides, a slight preference for glycine in position 6 of the common hexapeptide lead sequence cyclo(-Arg[1]-Gly[2]-Asp[3]-Phe[4]-Xaa[5]-Yaa[6]-) can be observed in both tests.

In the rank order of activity of the hexapeptides, the D-Ala[6]-containing peptides show a moderately decreased activity in assay A, with IC_{50} values of 0.14 and 0.19 μM for compounds **4** and **3**, respectively. These peptides are followed by the L-Pro- and D-Pro-containing hexapeptides **5**, **6**, **7** and **8**, with activities in the range of approximately 0.25–1.0 μM for test system A. Here, the previously detected slight preference for glycine in position 6, i.e., preceding Arg[1], is altered in favour of the side chain-bearing alanine. This preference is qualitatively supported by the results of bioassay B. Peptides **6** and **8** are more active than their Gly[6]-containing counterparts **5** and **7**.

The D-Arg[1]-containing peptides **1** and **2** are two orders of magnitude less active than the most active D-Phe[4]-containing peptides **11** and **12** in both tests. These peptides, as well as most of the cyclic pentapeptides, show a graded biological profile that qualifies them as appropriate candidates for comparative studies in order to identify pharmacophoric molecular substructures.

Comparable to the D-Arg[1]-containing hexapeptides **1** and **2**, the cyclic pentapeptide **13**, cyclo-(-D-Arg[1]-Gly[2]-Asp[3]-Phe[4]-Val[5]-), is two orders of magnitude less active when compared to the D-

TABLE 1
INHIBITORY CAPACITIES (IC_{50} VALUES) OF SYNTHETIC PEPTIDES AND PROTEIN LIGANDS AGAINST gpIIb/IIIa, EVALUATED IN TWO ALTERNATIVE SOLID-PHASE ASSAYS

Peptide	IC_{50} (10^{-6} M)	
	Assay A	Assay B
c(*R*GDFVA) **1**	4.2 ± 1.1	930 ± 100
c(*R*GDFVG) **2**	4.1	920 ± 11
c(RGDFV*A*) **3**	0.19 ± 0.06	33 ± 5.7
c(RGDFL*A*) **4**	0.14 ± 0.01	20 ± 2.3
c(RGDFPG) **5**	0.46 ± 0.18	36 ± 0.9
c(RGDFPA) **6**	0.26 ± 0.2	13 ± 0.6
c(RGDF*P*G) **7**	0.97 ± 0.24	82 ± 19
c(RGDF*P*A) **8**	0.43 ± 0.12	51 ± 3.9
c(RGD*F*VA) **9**	0.05 ± 0.01	7.6 ± 0.8
c(RGD*F*LA) **10**	0.17 ± 0.1	16 ± 1.2
c(RGD*F*VG) **11**	0.05 ± 0.01	5.3 ± 1.1
c(RGD*F*LG) **12**	0.03 ± 0.01	3.0 ± 0.3
c(*R*GDFV) **13**	3.9	410 ± 62
c(R*A*DFV) **14**	> 500	≫ 1200
c(RG*D*FV) **15**	25	> 800
c(RGD*F*V) **16**	0.23 ± 0.07	29 ± 5.8
c(RAD*F*V) **17**	101	> 1200
c(RGDF*V*) **18**	0.14 ± 0.09	16 ± 1.4
GRGDS	0.12 ± 0.05	10.5 ± 0.3
Fibrinogen	0.052 ± 0.01	–
Vitronectin	> 0.9	–
Fibronectin	0.23	–

In assay A the soluble integrin was preincubated with the peptide prior to adding it to the plastic-immobilized protein ligand, while the integrin was immobilized in assay B. The peptides are given in the one-letter notation; residues in D-configuration are underlined and in italics.

Phe[4]-containing hexapeptides **9**, **10**, **11** and **12**. Peptide **15**, containing a stereochemically inverted aspartic acid residue, is even less active. The most striking decrease in activity is found for the cyclic pentapeptides **14** and **17**, which both exhibit an additional methyl group on the C^{α} of position 2 within the recognition sequence. Both substitutions, either in the pro-*S* configuration in **17** or in the pro-*R* configuration in **14** of the original Gly[2], lead to a completely inactive peptide **14**, or at least to a dramatic drop in activity, when **17** is compared to its parent compound **16**. In test B both peptides, **14** and **17**, show no activity in the evaluated concentration range.

Peptides **16** and **18** are the only pentapeptides without any stereochemical or structural modifications within the essential recognition sequence and both demonstrate inhibitory activities comparable to the D-Ala[6]-containing cyclic hexapeptides **3** and **4**, which is a common trend in both assays. In general, all cyclic RGD peptides that contain an unmodified recognition sequence show nearly equal activities, with IC_{50} values in the ranges 0.1–1.0 and 10–100 μM for tests A and B, respectively. Only the D-Phe[4]-containing hexapeptides are slightly more active and reach inhibitory potentials comparable to soluble fibrinogen and fibronectin. Therefore, they should be capable to compete sufficiently with the native substrate for binding to gpIIb/IIIa. All of the pentapeptides are even less active than the standard linear peptide GRGDS, due to their modifications within the RGD sequence.

Peptide conformations

The conformations of most of the peptides investigated here have already been described in detail [14,34,58,59]. As mentioned above, they follow common structural templates constructed

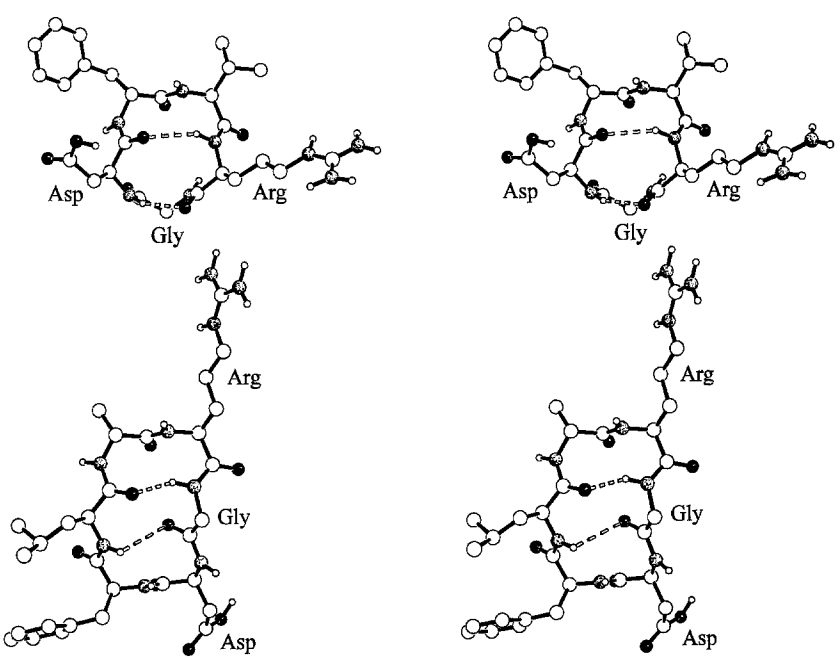

Fig. 1. Stereoplot of NMR-refined conformations of RGD peptides. Oxygen atoms are black, nitrogen atoms are stippled. Intramolecular hydrogen bonds are indicated with broken lines. Top: in c(RGD*F*V), **16**, the recognition tripeptide forms a tight γ turn. Bottom: the RGD sequence adopts an almost extended conformation in c(RGDFL*A*), **4**.

by two reverse-turn modules. The cyclic hexapeptides adopt a two-β-turn conformation, characterized by a pair of intramolecular hydrogen bonds between residues i and i+3, whereas the cyclic pentapeptides form a βII' γ-turn conformation [12,14]. In both structural families the D-amino acid induces a βII' turn by adopting the i+1 position. The refined conformations of peptides **16** and **4** are depicted in Fig. 1 in order to address the question of the available conformational space for the tripeptide sequence Arg-Gly-Asp, when incorporated and oriented in different positions within the two templates.

TABLE 2
VECTOR ANALYSIS CARRIED OUT FOR STRUCTURES OF THE NMR-REFINED Arg-Gly-Asp PEPTIDES, THE SNAKE VENOMS ECHISTATIN AND KISTRIN AND SELECTED Arg-Xaa-Asp-CONTAINING PROTEIN STRUCTURES FROM THE BROOKHAVEN PDB

Peptide/protein		$r^{\alpha\alpha}$ (nm)	$r^{\beta\beta}$ (nm)	μ (°)	ν (°)	φ (°)
c(*R*GDFVG)	**2**	0.523	0.725	152	102	−162
c(RGDFV*A*)	**3**	0.640	0.890	147	142	21
c(RGDFL*A*)	**4**	0.694	0.941	146	142	7
trans-c(RGDFPG)	**5**	0.631	0.811	120	132	0
cis-c(RGDFPG)	**5**	0.541	0.692	141	102	17
trans-c(RGDFPA)	**6**	0.626	0.794	119	127	0
cis-c(RGDFPA)	**6**	0.547	0.735	152	107	32
c(RGDF*P*G)	**7**	0.644	0.880	133	149	−13
c(RGD*F*VA)	**9**	0.569	0.776	159	111	36
c(RGD*F*LA)	**10**	0.547	0.699	142	99	39
c(RGD*F*VG)	**11**	0.613	0.873	169	132	26
c(RGD*F*LG)	**12**	0.565	0.740	139	112	20
c(*R*GDFV)	**13**	0.566	0.823	169	129	102
c(R*A*DFV)	**14**	0.600	0.725	114	114	−10
c(RGD*F*V)	**16**	0.547	0.668	113	113	−6
c(RAD*F*V)	**17**	0.512	0.744	139	139	5
c(RGDF*V*)	**18**	0.658	0.905	139	144	−15
ECHI-1		0.657	0.754	86	133	−23
ECHI-2		0.881	1.102	126	145	−35
ECHI-3		0.697	0.953	158	133	81
ECHI-4		0.724	0.977	149	137	−81
ECHI-5		0.628	0.785	115	121	−65
ECHI-6		0.570	0.545	87	79	45
ECHI-7		0.642	0.792	157	88	66
ECHI-8		0.540	0.726	162	101	37
Kistrin		0.623	0.853	132	145	−23
1GCR		0.717	0.902	123	131	8
7TLN		0.621	0.834	155	116	−56
1CC5		0.510	0.654	143	85	119
1CD4		0.681	0.802	135	81	−126
2ALP		0.557	0.715	158	84	151
1CCR		0.553	0.746	152	102	134
TEN		0.614	0.778	116	127	−33

For the cyclic peptides the one-letter notation is used. Amino acids in D-configuration are marked with underlined italics. $r^{\alpha\alpha}$ and $r^{\beta\beta}$ refer to the Arg C^{α}-Asp C^{α} and Arg C^{β}-Asp C^{β} distances, respectively. The angles μ, ν and the pseudodihedral angle φ are denoted in relation to Fig. 3. The protein structures taken from the Brookhaven PDB are named by the usual four-letter notation: 1GCR = γ-crystalline [60], 7TLN = thermolysin [84], 1CC5 = cytochrome c [85], 1CD4 = T-cell surface protein [86], 2ALP = alpha-lytic protease [87], 1CCR = cytochrome c [88], TEN = tenascin [89].

In Fig. 1 (top) the RGD sequence is arranged in a tight γ-turn conformation, with Gly^2 in the i+1 position of the γ turn and D-Phe^4 in the i+1 position of the βII' turn. The γ turn enables the peptide backbone to form a bend at Gly^2 and to reverse the chain direction within the recognition sequence. In contrast to this particular bent RGD conformation, the tripeptide adopts an almost extended structure in the cyclic hexapeptide **4** (Fig. 1, bottom). The D-Ala^6-containing hexapeptides have been designed in order to expose the RGD sequence in a manner comparable to a strand of a β-sheet structure as found in the protein γ-crystalline [60].

From a conformational point of view, the two peptides **16** and **4** represent the geometrical extremes as far as the RGD sequence is concerned. The tripeptide is found in the tightest possible turn (**16**) and in the most extended conformation (**4**) possible in the underlying templates. The rms deviation of 0.22 nm for superpositioning all heavy atoms of the essential recognition tripeptide sequence of **16** and **4** shows the conformational difference between both peptides. The extended character of the RGD tripeptide conformation of **4** is clearly defined by the Arg^1C^α-Asp^3C^α and Arg^1C^β-Asp^3C^β distances. Among all synthetic RGD peptides discussed here, compound **4** displays the maximum values for both distances ($r^{\alpha\alpha}$ = 0.694 nm, $r^{\beta\beta}$ = 0.941 nm, Table 2), while for the pentapeptide **16** these distances are close to the corresponding minimum values ($r^{\alpha\alpha}$ = 0.547 nm, $r^{\beta\beta}$ = 0.668 nm, Table 2). Although both peptides are designed based on different templates, and display the most different RGD conformations when compared to each other, they have nearly identical biological activities in the gpIIb/IIIa binding test (Table 1). This somewhat contradictory finding will be addressed in the Discussion section. The D-Phe^4-containing cyclic hexapeptides show the highest activities in the platelet surface receptor binding assay; their structures are presented in Fig. 2.

The superposition of the four hexapeptides **9–12** with respect to their backbone atoms supports the common βII', βII conformation, with D-Phe^4 in the i+1 position of βII' turns and Arg^1-Gly^2 occupying the i+1 and i+2 positions of the βII turns. The conformational differences of these peptides are of minor importance, since they mainly affect β-turn distortions due to external γ turns, which are commonly due to simulation artifacts [61]. Focussing our interest on the essential

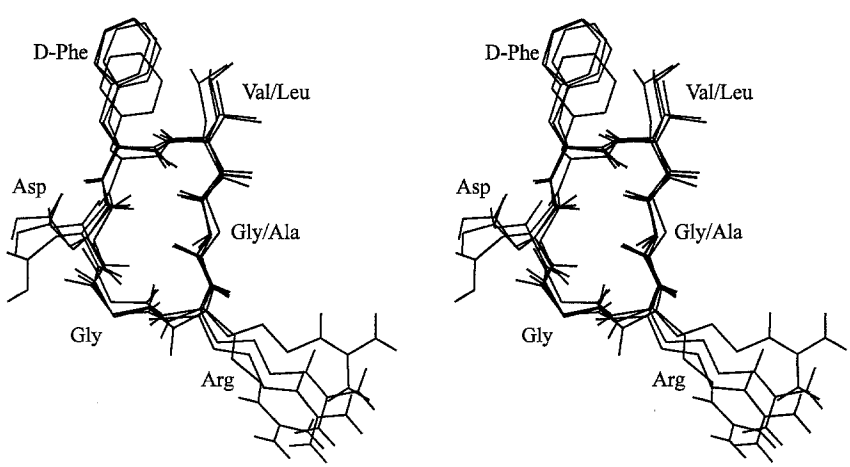

Fig. 2. Stereopresentation of a superposition of the refined D-Phe^4-containing cyclic hexapeptides **9–12**. Only the backbone atoms have been used for superimposing the four conformations.

RGD sequence, all D-Phe[4]-containing hexapeptides exhibit an almost identical pharmacophore arrangement with the Arg[1] and Asp[3] side chains in the i+1 and i+3 positions of a βII turn, respectively.

Vector analysis

A vector analysis over all conformationally analyzed RGD peptides, the conformations of echistatin [52] and kistrin [51], and selected Arg-Xaa-Asp-containing protein structures was carried out to derive geometrical descriptors that could possibly correlate with the activity profile of the RGD peptides. In a procedure similar to the CAVEAT program developed by Bartlett et al. [50], the relative orientations of two vectors were analyzed for all the structures given in Table 2.

This geometry pattern analysis has been previously utilized by Bogusky et al. [62], who compared conformations of two Arg-Gly-Asp-containing pentapeptides bridged by disulfide bonds with respect to their activity as fibrinogen receptor antagonists. In a further comparative study of a variety of homo- and heterodetic cyclic RGD peptides, Peishoff et al. [63] defined a different set of geometrical descriptors to categorize observed backbone conformations. They classified different structure types by analyzing angles between two consecutive C^{α}-C^{α} vectors. We decided to choose the C^{α}-C^{β} bonds of Arg[1] and Asp[3] as relevant vectors, because their orientation is mainly responsible for exposing the essential side-chain functionalities and therefore they should determine the pharmacophore geometry. In addition, the orientation of these vectors is not affected by variations of side-chain torsions that certainly occur during the receptor-binding event. We will restrict the discussion of side-chain exposure to these two vectors, since their orientation can be determined by means of NMR-derived structural analysis with a high degree of confidence. The parameters that describe the relative orientation of the vector pair are explained in Fig. 3.

From the vector analysis it is obvious that the C^{α}-C^{α} distances $r^{\alpha\alpha}$, the C^{β}-C^{β} distances $r^{\beta\beta}$ and both C^{β}-C^{α}-C^{α} angles are in a comparable range for all peptides and proteins (Table 2). Fixing the RGD sequence in cyclic hexa- and pentapeptide templates restricts the C^{β}-C^{β} distance which is in the range of 0.668 to 0.941 nm for the synthetic peptides, whereas it spreads between 0.545 and 1.102 nm for the proteins. A more striking difference is found for the pseudodihedral angle

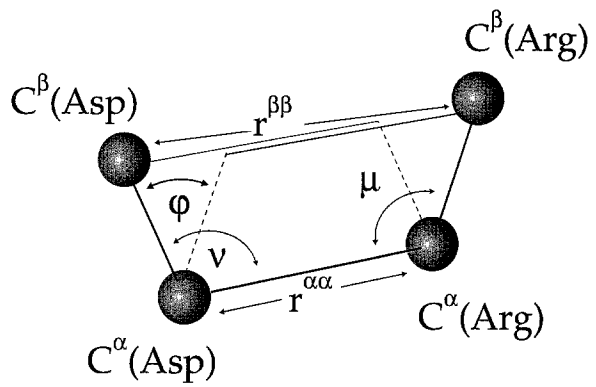

Fig. 3. Definition of the geometrical parameters used for the structure analysis given in Table 2. The C^{α} and C^{β} atoms of Arg[1] and Asp[3] are symbolized as shaded balls. The notation for the distance vectors, angles and the pseudodihedral angle is used throughout the text.

φ that describes the torsional orientation of both vectors. The protein structures populate the complete conformational space with respect to φ and no preference can be derived for this parameter. Excluding the D-Arg- and D-Asp-containing RGD peptides, the mean value over the RGD peptide conformations is $\langle\varphi\rangle = 11 \pm 17°$. All of the cyclic RGD peptides containing L-Arg and L-Asp cover an extremely restricted area of conformational space that is uniformly populated by the proteins, as indicated by the φ dihedral.

A model MD simulation was carried out for Ac-Gly-Arg-Gly-Asp-Phe-Gly-$NHCH_3$ over 500 ps at a temperature of 1000 K in order to investigate the conformational space principally accessible to the vector pair within a linear RGD peptide. These geometrical parameters are followed over the 500 ps trajectory with 2000 snapshots in Fig. 4.

The two distance parameters $r^{\alpha\alpha}$ and $r^{\beta\beta}$ are governed by covalent restrictions to a limited distance range. Interestingly, the pseudodihedral angle φ shows no preferred values but covers the entire torsional space uniformly; a result which is similar to that indicated by the analysis of the protein structures.

This observation, especially the obvious restriction of φ in the cyclic peptides, will be discussed in detail with respect to the activities in the following section.

DISCUSSION

From a thorough inspection of the inhibitory activities (Table 1) of the discussed RGD peptides it becomes obvious that the differences in biological activity are moderate. Nevertheless, we consider it reasonable to postulate hypothetical pharmacophore geometries based on the presented structural and biological data.

Ala^2-containing peptides

When evaluating the binding affinities derived by the two methodologically different solid-phase assays A and B of the cyclic hexa- and pentapeptides given in Table 1, it becomes obvious that the $Gly^2 \rightarrow$ (L,D)-Ala^2 modified peptides exhibit the most striking effect in relation to the ensemble of compounds investigated here. While the D-Ala^2-containing pentapeptide **14** is absolutely inactive in both assays, the L-Ala^2-containing peptide **17** is less active in assay A than the

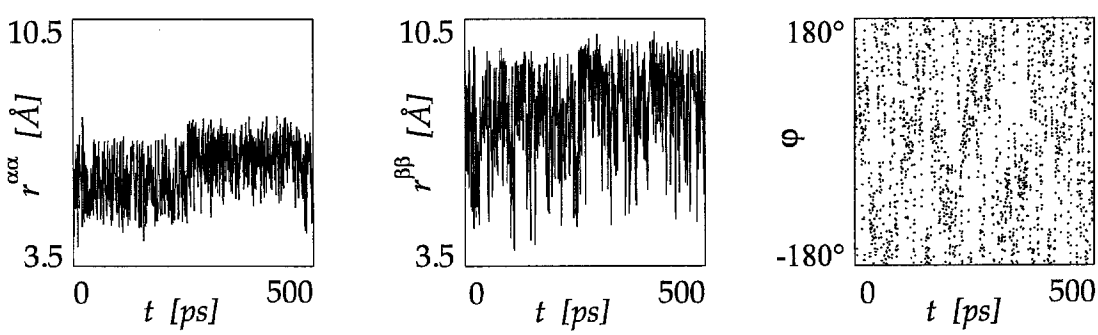

Fig. 4. Analysis of the 500 ps MD simulation of Ac-Gly-Arg-Gly-Asp-Phe-Gly-$NHCH_3$ at 1000 K. The C^{α}-C^{α} (left) and C^{β}-C^{β} (middle) distances between Arg^1 and Asp^3 and the connecting pseudodihedral angle φ (right) are monitored over 2000 snapshots.

unmodified parent peptide **16** by a factor of approximately 450, and completely inactive in assay B. In principle, two possible explanations can account for this dramatic drop in activity of the Arg-(D,L)-Ala-Asp pentapeptides. Firstly, the additional methyl substituent in position 2 of the essential recognition tripeptide sequence restricts the inherent conformational space in such a way that the required receptor-fitting arrangement of the arginine and aspartic acid side chains cannot be formed. Secondly, the additional methyl group in peptides **14** and **17** prevents tight receptor binding by repulsive interactions with receptor residues that probably form a sterically demanding binding pocket for an unsubstituted backbone in the center of the recognition sequence. By a pairwise comparison of the Arg-Ala-Asp peptides **14** and **17** with conformationally related Arg-Gly-Asp peptides, we can clearly rule out the first alternative of unfavourable conformational restriction within the essential tripeptide sequence. Peptide **14** adopts the designed βII' γ conformation, with a βII' turn formed by the sequence Arg[1]-D-Ala[2]-Asp[3]-Phe[4]. A similar turn geometry for that particular sequence is found in the all-trans conformations of the L-Pro-containing hexapeptides **5** and **6**, as well as in the D-Pro-containing hexapeptide **7** (compound **8** could not be analyzed, due to severe signal overlap in the 2D NMR spectra). In these hexapeptides the same type-II' β turn is formed. The structural superposition of the residues Arg[1]-Gly[2]/D-Ala[2]-Asp[3]-Phe[4] of peptides **7** and **14** stresses the conformational similarity between the inactive peptide **14** and the highly active proline-containing compounds **5**–**8**, as far as the potential pharmacophoric residues are concerned (Fig. 5).

Keeping in mind this close structural relationship, the methyl substitution in pro-*R* configuration at Gly[2] in **14** does not prevent the formation of a backbone conformation that allows for receptor binding, as confirmed by the analysis of the structures of *trans*-**5**, *trans*-**6** and **7** [59].

Even more impressive is the almost structural identity of the L-Ala[2] peptide **17** with the parent peptide **16** (Fig. 6, Table 3). A slight difference is found for the ψ dihedral angle of Arg[1] and both ϕ and ψ of Asp[3]. In **17** these angles adopt values that account for a more extended conformation flanking the reverse γ turn. Nevertheless, an identical pharmacophore can be exposed for both pentapeptides. Once again, the methyl substituent in pro-*S* orientation of an unmodified

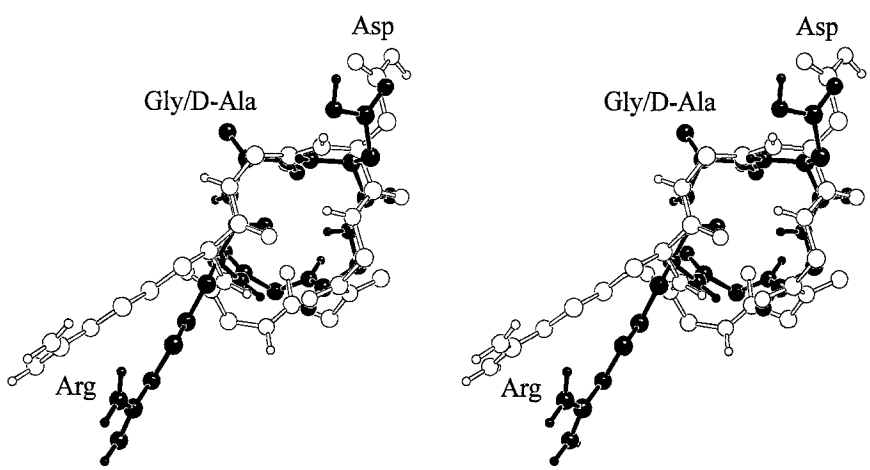

Fig. 5. Stereoplot of the structural superposition of c(R*A*DFV), **14** (black), and c(RGDF*P*G), **7** (white), with respect to their common βII' turn (shown in the upper part). Only the side chains of residues Arg[1] and Asp[3] are shown.

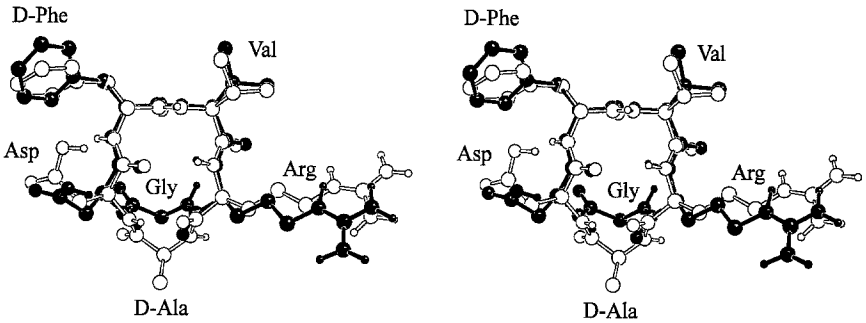

Fig. 6. Stereoplot of the structural superposition of c(RGD*F*V), **16** (black), and c(RAD*F*V), **17** (white), with respect to the backbone atoms of residues Asp[3], D-Phe[4], Val[5] and Arg[1].

Gly[2] does not prevent the formation of a potential pharmacophore geometry that is present in the Arg-Gly-Asp peptide **16** which is 500 times more active than the methyl analogue **17** in assay A, while **17** is inactive in assay B.

As a consequence of these indirect comparative studies, we propose as working hypothesis that any substitution on the C^{α} atom of Gly[2] creates major steric conflicts within the binding pocket of gpIIb/IIIa. Whether in the pro-*R* or in the pro-*S* orientation, the additional substituent occupies an excluded receptor volume which therefore prevents efficient receptor binding. This proposed highly restrictive steric demand of the platelet receptor gpIIb/IIIa will be of prime importance for pseudoreceptor modelling studies, based on a series of platelet-associated receptor antagonist structures, that are in progress in our group. We postulate a narrow binding cleft for the central Gly[2] residue of the substrates that does not tolerate any further substituents on the C^{α} atom.

A different steric demand with respect to Gly[2] modifications was previously proposed for the vitronectin and laminin fragment P1 receptors, based on inhibition studies of tumor cell adhesion

TABLE 3
DIHEDRAL ANGLE COMPARISON FOR THE CONFORMATIONALLY RELATED CYCLIC PENTAPEPTIDES c(RGD*F*V) AND c(RAD*F*V)

Residue	ϕ (°)	ψ (°)	ω (°)	Turn	Position
c(RGD*F*V) **16**					
Arg[1]	−128	73	−179		
Gly[2]	88	−66	169	γ	i+1
Asp[3]	−85	81	−172		
D-Phe[4]	85	−111	178	βII'	i+1
Val[5]	−58	−46	−178	βII'	i+2
c(RAD*F*V) **17**					
Arg[1]	−139	118	178		
Ala[2]	68	−58	164	γ	i+1
Asp[3]	−125	149	−175		
D-Phe[4]	68	−105	176	βII'	i+1
Val[5]	−86	−39	−178	βII'	i+2

The torsions are analyzed over MD-averaged and minimized structures, refined in a DMSO solvent box. Additional to the torsion values, the amino acids are characterized with respect to their position within turns.

with the same peptides as discussed here [14]. In this investigation we proposed that the integrins involved tolerated a methyl substituent in pro-*S* orientation of the Gly^2 C^{α} atom, whereas substitution in pro-*R* configuration leads to an absolutely inactive peptide. Interestingly, Arg-Ala-Asp peptide **17** was one of the few compounds tested which exhibited remarkable inhibitory potential against vitronectin-mediated tumor cell adhesion [14,34,58].

Taking these facts together, we conclude that the tumor cell-associated laminin fragment P1 and vitronectin receptors differentiate between pro-*R* and pro-*S* orientations of substituents at the Gly^2 C^{α} atom, such that only the pro-*R* volume is restricted by the binding site of the integrins, whereas the platelet-associated $\alpha_{IIb}\beta_3$ integrin forms a narrow cleft which can only be occupied by an unsubstituted linker connecting Arg^1 and Asp^3.

D-Arg^1-, D-Asp^3-containing peptides

To further refine a rough hypothetical model of the steric requirements that govern high-affinity binding to gpIIb/IIIa, we expand the comparative analysis from the central Gly^2 to its flanking residues, Arg^1 and Asp^3. In terms of receptor binding, all stereochemical modifications affecting Arg^1 and Asp^3 lead to peptides with remarkably reduced affinity. While all D-Arg^1-containing peptides, **1**, **2** and **13**, are still active in the micromolar and millimolar ranges in assays A and B, respectively, the D-Asp^3-containing pentapeptide **15** is one order of magnitude less active in assay A. We assume that the effect of inversion of Arg^1 chirality from L to D on side-chain orientation may be partially compensated by the reorientation of the four torsional angles along the arginine side chain. Therefore, the still remarkable activity of D-Arg^1-containing peptides could be rationalized by the fact that the guanidino functionality can still be presented in the appropriate receptor-complementary manner by exploiting the large conformational flexibility of the side chain, even though the C^{α} chirality is inverted with respect to the natural substrates.

This hypothesis is supported by previous investigations of small Arg-Gly-Asp peptide fibrinogen receptor antagonists. Samanen and co-workers [33] published a study of a series of cyclic pentapeptide disulfide analogues incorporating the recognition tripeptide. They have shown that for example the D-Arg-containing pentapeptideamide Ac-Cys-D-Arg-Gly-Asp-Pen-NH_2 (Pen = penicillamine), as well as the corresponding homo-arginine analogue Ac-Cys-hArg-Gly-Asp-Pen-NH_2 (hArg = homo-arginine) are more active than linear Ac-Arg-Gly-Asp-Ser-NH_2 in in vitro assays against gpIIb/IIIa by a factor of approximately 20. Although the arginine is stereochemically or constitutionally modified in both compounds, the recognition sequence is still capable of presenting an appropriate receptor-complementary pharmacophore geometry, probably due to the torsional freedom in the D-Arg and hArg side chains, respectively.
Obviously, this compensating mechanism does not allow a conformational reorientation of the configurationally inverted Asp^3 in **15**. This assumption explains the one order of magnitude lower IC_{50} values of the D-Arg^1-containing cyclopeptides **1**, **2** and **13** compared to the D-Asp^3-containing pentapeptide **15** in assay A.

Arg^1, Asp^3 side-chain orientation

The unexpected result that all peptides without modification in configuration and/or constitution within the Arg^1-Gly^2-Asp^3 recognition sequence show binding affinities in a narrow range of IC_{50} values (between 10^{-7} and 10^{-6} M in assay A and between 10^{-5} and 10^{-4} M in assay B), even though they have been designed utilizing different positioning within the different template

structures, requires the definition of a common conformational characteristic. In the following we wish to further refine the pharmacophore model proposed in Ref. 64 with respect to the relative orientation of the Arg^1 and Asp^3 side chains.

Both the cyclic hexapeptide template and the pentapeptide template can be described as having an almost flat backbone structure, with their C^α atoms nearly in a common plane [11,12]. Only the C^α atom of the i+1 residue of the γ turn within the pentapeptides deviates markedly from the plane spanned by the four remaining C^α atoms of the peptide (Fig. 6). All of the L-amino acids orient their side chains in the same direction with respect to this approximately defined plane, while D-residue side chains are exposed on the opposite side. The gpIIb/IIIa binding data of all L-Arg^1-Gly^2-L-Asp^3 peptides are in a narrow IC_{50} range, supporting the model of a common orientation of the carboxylate-bearing Asp^3 and the guanidino-bearing Arg^1 side chains within the same spatial area relative to the peptide ring plane. The correlation of the biological data with the vector analysis supports not only this particular relative orientation, but also a nearly parallel alignment of both side chains, as the pseudodihedral angle φ is found at values close to 0° for all unmodified recognition sequence-containing peptides (Table 2). All of the compounds with a stereochemically altered Arg^1-Gly^2-Asp^3 sequence show decreased binding affinities and expose their side chains with φ values greater than 100° (Tables 1 and 2). The analysis of the Arg-Xaa-Asp-containing protein structures and the results of the structure refinements of echistatin [52] and kistrin [51] clearly demonstrate that this restricted behaviour of φ in all L-Arg^1-Gly^2-L-Asp^3 peptides is not of covalent origin. This is supported by 500 ps of high-energy MD simulation of Ac-Gly-Arg-Gly-Asp-Phe-Gly-NHMe. During this simulation the completely available conformational space for φ is almost uniformly populated (Fig. 4). We therefore conclude that there is no major tripeptide-inherent conformational preference regarding φ. This finding is in agreement with the work of Cotrait et al. [64], who analyzed 48 Arg-Xaa-Asp fragments found in crystallographically refined protein structures and distinguished three main structural patterns describing the relative orientation of the arginine and aspartic acid side chains. In class I, they found a salt bridge between both functionalities which was previously defined by Siahaan et al. [65] as relevant for biological activity. These results were, however, based upon the conformational analysis of a cyclic Arg-Gly-Asp oligopeptide refined by molecular mechanics simulations in vacuum. In the protein structures these bridged Arg-Xaa-Asp sequences are mostly an integral part of the protein architecture and contribute to the stabilization of the overall tertiary structure through their electrostatic interactions. Thus, they do not represent a functionally relevant Arg-Gly-Asp recognition mimic. In class III proteins defined by Cotrait et al. [64], an elongated conformation was identified with both side chains oriented antiparallel, thus pointing in opposite directions. In this family of proteins, one of the functionally relevant side chains protrudes into the surrounding solvent, while the second side chain is found buried in the interior of the protein and is engaged in a network of hydrogen bonds. The members of this subclass cannot be considered as being representative of adhesive proteins, since the recognition sequence has to be surface exposed in order to bind to the receptor subsite. However, the identified characteristics of class II Arg-Xaa-Asp conformations agree with our findings derived from the conformationally constrained oligopeptides. The side chains of arginine and aspartic acid are found exposed on the protein surface and point in a parallel direction. The members of this family can be seen as functionally relevant Arg-Gly-Asp representatives, which is supported by the fact that the biologically active protein γ-crystalline [66] is a member of this class. The unique folding pattern has been described

as a 'U-shape', formed by the elongated arginine side chain, the glycine backbone and the aspartic acid side chain [64]. On the basis of our analysis of peptide structures, we further refine this U-shaped arrangement to a U form with a *kinked bottom curve*, represented by the glycine backbone, that deviates from the plane of a regular U (Fig. 7).

The results of this protein structure survey confirm the validity of our procedure and enable us to propose a preliminary pharmacophore model on the basis of low-molecular-weight Arg-Gly-Asp peptide structures by comparative studies.

Significance of the residue following the RGD tripeptide

Apart from these substantial conformation–activity relationships, derived from comparative analyses of refined structures of constrained peptides, we wish to discuss the significance of the residue following Asp^3, which does not play such a critically important role as Arg^1 or Asp^3 modifications. Nevertheless, when examining the inhibition constants of all of the peptides in both assays, a clear preference for phenylalanine in D-configuration in this position can be postulated, since the D-Phe^4-containing hexapeptides **9**–**12** are the most active ones. This cannot

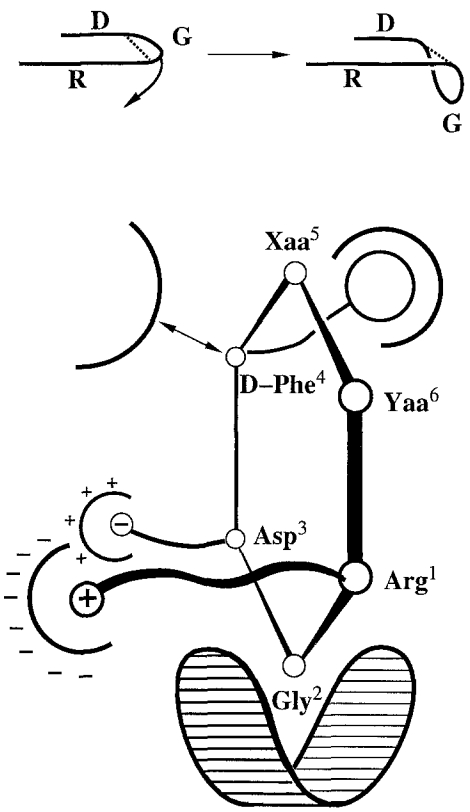

Fig. 7. Schematic representation of the qualitatively derived pharmacophore requirements of gpIIb/IIIa. Top: the previously postulated U-shaped contour (left) for the Arg^1 side chain-Gly^2 backbone-Asp^3 side-chain path is further refined to a U-shape with a kinked bottom curve (right). Bottom: qualitative presentation of the steric and electronic requirements of the binding pocket around a cyclic hexapeptide, symbolized by a regular six-membered ring. The tight binding pocket around Gly^2 is given at the bottom.

exclusively arise from a unique favourable Arg-Gly-Asp conformation for gpIIb/IIIa binding within these compounds. Structural comparison of these peptides with the L- and D-Pro-containing hexapeptides **5**–**7** allows us to identify almost identical substructures for the recognition sequence, and these peptides exhibit moderately decreased activities (Table 1). In the D-Phe^4 hexapeptides **9**–**12**, the essential tripeptide sequence forms a βII turn with Arg^1 and Gly^2 in the i+1 and i+2 positions, respectively. In the cis conformations of the L-Pro-containing peptides **5** and **6** an identical conformation was analyzed, as described recently [59]. The all-trans conformations of these peptides, as well as the refined structure for **7**, expose the essential tripeptide in the i, i+1 and i+2 positions of a βII' turn [59]. Although a positional shift exists within the common hexapeptide template when comparing for example **7** with the D-Phe^4-containing hexapeptides, the tripeptide conformation is quite similar to the kinked backbone trace, with Gly^2 in a hinge position. In both peptide classes Gly^2 occupies either the i+1 (**7**, *trans*-**5**, *trans*-**6**) or the i+2 (**9**–**12**, *cis*-**5**, *cis*-**6**) position of a reverse β turn and induces a bend in the tripeptide sequence. It is therefore possible to find peptides with an Arg-Gly-Asp conformation related to those of the D-Phe^4-containing hexapeptides. These conformationally related compounds show a differentiated and moderately decreased activity, which indicates the significance of a further structural element, positively contributing to receptor binding for **9**–**12**. We assign this additional contribution to the D-configuration of Phe^4 within these peptides. Therefore, we propose a favourable hydrophobic binding site on the opposite face of the Arg^1 and Asp^3 side-chain orientations relative to the peptide ring plane (Fig. 7). This pocket can only be occupied by residues exposing their side chains to the backface of the peptide templates when viewed from the direction of the L-residue side chains. Alternatively, this could also be accounted for by a resolved steric conflict between a residue in L-configuration at position 4 of the peptides **9**–**12** and an excluded receptor volume in this spatial area, but in this case the difference in binding affinities for all L-Phe^4-containing peptides compared to the D-Phe^4-containing compounds should be more distinct. Nevertheless, we found a clear tendency in biological activity favouring the D-Phe^4-containing hexapeptides, which can hypothetically be rationalized in terms of the postulated pharmacophore model outlined above (Fig. 7). This particular finding is partially supported by a recently published investigation of a series of cyclic nonapeptides following the general primary sequence -Xaa-Gly-His-Arg-Gly-Asp-Yaa-Arg-Cys-, where Xaa represents a residue capable of forming a disulfide linkage with the C-terminal cysteine residue, e.g., Pen, Pmc, Pmp or Tmc (Pmc = β,β-pentamethylenecysteine; Pmp = β,β-pentamethylene-β-mercaptopropionic acid; Tmc = β,β-tetramethylenecysteine) [36]. The authors investigated a series of 11 peptides which had been prepared in order to study the influence of the amino acid Yaa following the recognition tripeptide on gpIIb/IIIa binding affinity. It was found that highly hydrophobic and aromatic residues resulted in increased binding. Substitution of for example leucine against Tyr(*O*-*n*-butyl) resulted in an enhancement of receptor binding by one order of magnitude [36]. Unfortunately, in this work only a two-dimensional representation of the essential Arg-Gly-Asp-Yaa pharmacophore was elaborated, since no conformational studies have been carried out on these peptides. Nevertheless, the finding supports qualitatively the existence of a hydrophobic binding pocket, which probably can accommodate both the D-Phe^4 side chain of the hexapeptides **9**–**12** and the Yaa side chains of the cyclic nonapeptide disulfides. The increased conformational flexibility of a cyclic nonapeptide when compared to our hexapeptide template may account for a similar spatial orientation of the Yaa residues in L-configuration as determined by us for D-Phe^4 of **9**–**12**.

Interestingly, the D-Phe^4-containing pentapeptide **16** is not as active as, for example, **12**. This can be explained by the more restricted conformation of the essential tripeptide, which is arranged in a unique, tightest possible turn geometry in this pentapeptide (Fig. 6). No other compound shows a comparably short C^{β}-C^{β} distance of $r^{\beta\beta}$ = 0.668 nm, together with μ and ν angles of around 110° (Table 2). This peptide cannot present a comparable extended conformation for the Gly^2-Asp^3-D-Phe^4 sequence, in contrast to the D-Phe^4-containing hexapeptides. The Asp^3 residue of **16** adopts an inverse γ conformation with $\phi = -85°$ and $\psi = 81°$, whereas for the two most active hexapeptides, **11** and **12**, the Asp^3 residue is found in a more extended backbone structure, i.e., Asp^3(**11**): $\phi = -130°$, $\psi = 120°$; Asp^3(**12**): $\phi = -123°$, $\psi = 120°$.

This finding is not in agreement with a recently published comparative study of a series of homo- and heterodetic cyclic Arg-Gly-Asp peptides, refined by means of NMR spectroscopy and X-ray crystallography [63,67,68]. In this investigation the authors defined four structurally distinct categories, according to the conformational preference of the recognition tripeptide backbone. The angle between consecutive C^{α}-C^{α} vectors, centered at each amino acid of the tripeptide, was analyzed in terms of a geometrical descriptor [63]. The most active compounds, for example Ac-Cys-(N^{α}-Me)Arg-Gly-Asp-Pen-NH_2 (SK&F 106760) and Mba-(N^{α}-Me)Arg-Gly-Asp-Man (SK&F 107260) (Mba = 2-mercaptobenzoic acid; Man = 2-mercaptoaniline), adopt a *turn-extended-turn* Arg-Gly-Asp conformation with arginine and aspartic acid in a locally kinked conformation and glycine in an extended structure. This particular arrangement corresponds to that of the D-Ala^6-containing peptides **3** and **4** discussed by us, that expose the essential tripeptide in the same manner. In contrast to the results of our D-Phe^4 peptides **9–12**, a closely related analogue, notably cyclo(-Arg^1-Gly^2-Asp^3-D-Pro^4-Pro^5-Gly^6-) is found to be inactive [67]. The structure of this peptide is described by an Arg-Gly β-turn conformation where the arginine and glycine residues occupy the i+1 and i+2 positions of a type-II β turn, identical to the analyzed structures of all of the D-Phe^4 hexapeptides described above. The authors explain the missing antagonistic activity of the D-Pro^4-containing peptide by means of comparative modelling with an unfavourable volume distribution of the non-RGD residues, D-Pro^4-Pro^5-Gly^6, relative to the recognition sequence [63]. Steric repulsive interactions with the receptor are defined as being significant for the prevention of receptor binding of this peptide. In this context, the structural and biological data of **9–12** disprove this hypothesis to a certain extent. The D-Phe^4 hexapeptides are conformationally almost identical to the above-mentioned D-Pro^4 analogue and show the highest activities in our investigation. As remarkable structural difference, the restricted character of the D-Pro^4-Pro^5 side chains may account for interactions with excluded receptor volumes on gpIIb/IIIa. The D-Phe^4-Val^5-(Leu^5) fragment of the cyclic hexapeptides discussed here can probably resolve such steric conflicts by rotation of the χ^1 and χ^2 torsions.

This apparent contradiction aside, several conclusions drawn by Peishoff et al. [63] support our structure–activity studies. The most active peptides of their investigation expose the arginine and aspartic acid side chains in a nearly parallel manner within the *turn-extended-turn* category, while the $C^{\alpha}H_2$ group of the glycine spacer residue is easily accessible and may interact with a narrow groove on the receptor, as proposed in our pharmacophore model (Fig. 7).

After the first publication of the biological profiles of the peptides described here [69,70], a study by Hirschmann and co-workers appeared [71] in which three cyclic hexapeptides, cyclo-(-Arg-Gly-Asp-Phe-Phe-Gly-), cyclo(-Arg-Gly-Asp-D-Ser-Phe-Gly-) and cyclo(-Arg-Gly-Asp-D-Ser-Phe-D-Phe-), have been tested as gpIIb/IIIa antagonists. It turned out that two of them show

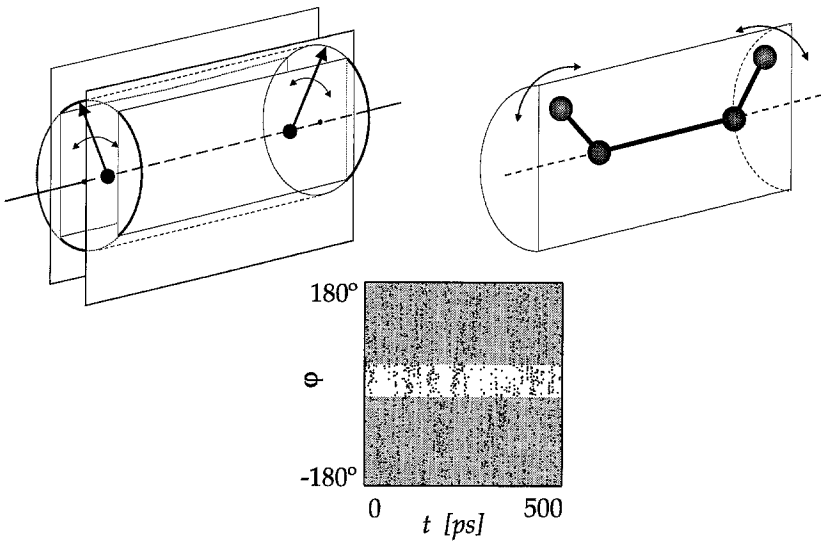

Fig. 8. Schematic representation of the filter effect applied to the torsional relation of the Arg[1] and Asp[3] C^{α}-C^{β} bonds. The effect is due to the utilization of cyclic hexa- and pentapeptide templates. The incorporation of the essential tripeptide sequence in cyclic hexa- and pentapeptides restricts the torsional freedom of φ to only a small section, with almost parallel aligned C^{α}-C^{β} bonds (top left). Within this section only angle fluctuations are allowed (top right). Compared to the principal conformational space for φ, the torsion angles in the analyzed cyclic peptides populate only values around 0°. The filter is symbolized by shaded regions of the trajectory analysis of φ (below).

submicromolar IC_{50} values in an ELISA gpIIb/IIIa–fibrinogen receptor assay. Unfortunately, the authors did not perform any conformational studies on these peptides, therefore we cannot use them for a comparison with our findings.

CONCLUSIONS

On the basis of a series of cyclic homodetic hexa- and pentapeptides containing the essential recognition sequence Arg-Gly-Asp, detailed structure–activity relationships regarding in vitro binding to the platelet-associated integrin gpIIb/IIIa could be derived by classical comparative studies, coupled with an indirect molecular design strategy. The approach of utilizing conformational restriction of substrate structures to indirectly obtain information about receptor requirements [11–13] is in any case superior to conformational analyses of flexible linear RGD peptides [72]. We hypothesize that the $\alpha_{IIb}\beta_3$ integrin has highly restrictive steric requirements regarding the Arg- and Asp-connecting structure element and the relative orientation of both side chains. The outlined results allow for further refinement of a pharmacophore model previously postulated in the literature [64], with special emphasis on the glycine $C^{\alpha}H_2$ orientation and accessibility (Fig. 7). It was possible to utilize systematically a geometrical descriptor scheme that allows for the correlation of conformational characteristics, notably the pseudodihedral angle φ, with the antagonistic activities of the compounds studied. This particular dihedral angle populated an unexpectedly restricted area of the principally available torsional range from −180 to +180°. This restriction was proven to be due to the incorporation of the recognition tripeptide into the underlying structural scaffolds. The combination of experimentally based structural analyses with

comparative studies of structures from the protein database and with model MD simulations provided a clear view of how the conformational space of RGD was governed by the utilization of selected structure templates. The utilization of cyclic hexa- and pentapeptides as scaffolds for two functionalities in a 1,3 relation acts like a filter on the conformational adjustment of 1,3-exposed side chains (Fig. 8) which are, in linear peptides, by no means restricted to a preferred area, as indicated by the protein structure survey and the high-temperature MD simulation of the linear model peptide (Figs. 4 and 8). This result should be kept in mind for future design studies which exploit cyclic peptidic frameworks for a controlled orientation of functionalities.

These reported findings should have major impact on the reconstruction of the receptor binding site by a pseudoreceptor modelling procedure. It was not the main purpose of this study to focus on the activities of the peptides, since the development of potential low-molecular-weight antithrombotic drugs is under active investigation in the pharmaceutical industry [33,38–40,63,73]. Rather, it has been our aim to demonstrate the potential of comparative studies, for example in the definition of differentiating recognition mechanisms of tumor cell-associated integrins on the one hand and gpIIb/IIIa on the other hand. We hope to have demonstrated the fidelity of the rational- and structural-oriented approach for deriving structure–activity relationships by means of comparative studies. Investigations of this type have to be seen complementary to the less structural-oriented strategies in drug design, such as random peptide libraries [74–81], the peptoid approach [82,83] and random screening studies.

ACKNOWLEDGEMENTS

Financial support of the Deutsche Forschungsgemeinschaft and the Fonds der Chemischen Industrie is gratefully acknowledged. M.G. thanks the Studienstiftung des Deutschen Volkes and G.M. the Fonds der Chemischen Industrie for doctoral fellowships. The technical assistance of Dr. G. Schnorrenberg (Boehringer Ingelheim KG) in providing peptide purification facilities and of Dr. W. König (Hoechst AG, Frankfurt am Main) in amino acid analysis is acknowledged, too. We thank Dr. Gordon Kennedy (Glaxo Verona) and Dr. Alan P. Tonge (Glaxo Greenford) for carefully reading the manuscript.

REFERENCES

1 Claasen, V. (Ed.) Trends in Drug Research, Elsevier, Amsterdam, 1990.
2 Marshall, G.R., In Beddell, C.R. (Ed.) The Design of Drugs to Macromolecular Targets, Wiley, New York, NY, 1992, pp. 1–24.
3 Rosen, M.K. and Schreiber, S.L., Angew. Chem., Int. Ed. Engl., 31 (1992) 384.
4 Van Duyne, G.D., Standaert, R.F., Karplus, P.A., Schreiber, S.L. and Clardy, J., Science, 252 (1991) 839.
5 Van Duyne, G.D., Standaert, R.F., Schreiber, S.L. and Clardy, J., J. Am. Chem. Soc., 113 (1991) 7433.
6 Weber, C., Wider, G., Von Freyberg, B., Traber, R., Braun, W., Widmer, H. and Wüthrich, K., Biochemistry, 30 (1991) 6563.
7 Fesik, S.W., Gampe Jr., R.T., Eaton, H.L., Gemmecker, G., Olejniczak, E.T., Neri, P., Holzman, T.F., Egan, D.A., Edalji, R., Simmer, R., Helfrich, R., Hochlowski, J. and Jackson, M., Biochemistry, 30 (1991) 6574.
8 Richards, W.G. (Ed.) Computer-Aided Molecular Design, Oxford University Press, London, 1989.
9 Perun, T.J. and Propst, C.L. (Eds.) Computer-Aided Drug Design, Methods and Applications, Marcel Dekker, New York, NY, 1989.
10 Kuntz, I.D., Science, 257 (1992) 1078.

11 Kessler, H., Haupt, A. and Will, M., In Perun, T.J. and Propst, C.L. (Eds.) Computer-Aided Drug Design, Methods and Applications, Marcel Dekker, New York, NY, 1989, pp. 461–483.
12 Kessler, H., Angew. Chem., Int. Ed. Engl., 21 (1982) 512.
13 Hruby, V., Life Sci., 31 (1982) 189.
14 Gurrath, M., Müller, G., Kessler, H., Aumailley, M. and Timpl, R., Eur. J. Biochem., 210 (1992) 911.
15 Gartner, T.K. and Bennett, J.S., J. Biol. Chem., 260 (1985) 11891.
16 Kloczewiak, M., Timmons, S., Lukas, T.J. and Hawigar, J., Biochemistry, 23 (1984) 1767.
17 Lam, S.C.-T., Plow, E.F., Smith, M.A., Andrieux, A., Ryckwaert, J.-J., Marguerie, G. and Ginsberg, M.H., J. Biol. Chem., 262 (1987) 947.
18 Nichols, A.J., Ruffolo Jr., R.R., Huffman, W.F., Poste, G. and Samanen, J., Trends Pharmacol. Sci., 13 (1992) 413.
19 Ruoslahti, E. and Pierschbacher, M.D., Science, 238 (1987) 491.
20 Hynes, R.O., Cell, 48 (1987) 549.
21 Albeda, S.M. and Buck, C.A., FASEB J., 4 (1990) 2868.
22 Humphries, M.J., J. Cell Sci., 97 (1990) 585.
23 Damsky, C.H. and Bernfield, M., Curr. Opin. Cell Biol., 2 (1990) 813.
24 D'Souza, S.E., Ginsberg, M.H. and Plow, E.F., Trends Biochem. Sci., 16 (1991) 246.
25 Pierschbacher, M.D. and Ruoslahti, E., Nature, 309 (1984) 30.
26 Pierschbacher, M.D. and Ruoslahti, E., Proc. Natl. Acad. Sci. USA, 81 (1984) 5985.
27 Yamada, K.M., J. Biol. Chem., 266 (1991) 12809.
28 Pierschbacher, M.D. and Ruoslahti, E., J. Biol. Chem., 262 (1987) 17924.
29 Gehlsen, K.R., Argraves, W.S., Pierschbacher, M.D. and Ruoslahti, E., J. Cell Biol., 106 (1988) 925.
30 Hautanen, A., Gailit, J., Mann, D.M. and Ruoslahti, E., J. Biol. Chem., 264 (1989) 1437.
31 Samanen, J., Ali, F.E., Romoff, T., Calvo, R., Sørensen, E., Bennett, D., Berry, D., Koster, P., Vasko, J., Powers, D., Stadel, J. and Nichols, A., In Giralt, E. and Andreu, D. (Eds.) Peptides 1990 (Proceedings of the 21st European Peptide Symposium), ESCOM, Leiden, 1991, pp. 781–783.
32 Nutt, R.F., Brady, S.F., Sisko, J.T., Ciccarone, T.M., Colton, C.D., Levy, M.R., Gould, R.J., Zhang, G., Friedman, P.A. and Veber, D.F., In Giralt, E. and Andreu, D. (Eds.) Peptides 1990 (Proceedings of the 21st European Peptide Symposium), ESCOM, Leiden, 1991, pp. 784–786.
33 Samanen, J., Ali, F., Romoff, T., Calvo, R., Sørensen, E., Vasko, J., Storer, B., Berry, D., Bennett, D., Strohsacker, M., Powers, D., Stadel, J. and Nichols, A., J. Med. Chem., 34 (1991) 3114.
34 Aumailley, M., Gurrath, M., Müller, G., Calvete, J., Timpl, R. and Kessler, H., FEBS Lett., 291 (1991) 50.
35 Scarborough, R.M., Naughton, M.A., Teng, W., Rose, J.W., Phillips, D.R., Nannizzi, L., Arfsten, A., Campbell, A.M. and Charo, I.F., J. Biol. Chem., 268 (1993) 1066.
36 Cheng, S., Craig, W.S., Mullen, D., Tschopp, J.F., Dixon, D. and Pierschbacher, M.D., J. Med. Chem., 37 (1994) 1.
37 Klein, S.I., Molino, B.F., Chu, V., Ruggeri, Z., Czekaj, M., Gardner, C.J., Newman, J. and Barrett, J.A., In Giralt, E. and Andreu, D. (Eds.) Peptides 1990 (Proceedings of the 21st European Peptide Symposium), ESCOM, Leiden, 1991, pp. 374–375.
38 Callahan, J.F., Bean, J.W., Burgess, J.L., Eggleston, D.S., Hwang, S.M., Kopple, K.D., Koster, P.F., Nichols, A., Peishoff, C.E., Samanen, J.M., Vasko, J.A., Wong, A. and Huffman, W.F., J. Med. Chem., 35 (1992) 3970.
39 Alig, L., Edenhofer, A., Hadváry, P., Hürzeler, M., Knopp, D., Müller, M., Steiner, B., Trzeciak, A. and Weller, T., J. Med. Chem., 35 (1992) 4393.
40 Greenspoon, N., Hershkoviz, R., Alon, R., Varon, D., Shenkman, B., Marx, G., Federman, S., Kapustina, G. and Lider, O., Biochemistry, 32 (1993) 1001.
41 Gan, Z.-R., Gould, R.J., Jacobs, J.W., Friedman, P.A. and Polokoff, M.A., J. Biol. Chem., 263 (1988) 19827.
42 Dennis, M.S., Henzel, W.J., Pitti, R.M., Lipari, M.T., Napier, M.A., Deisher, T.A., Bunting, S. and Lazarus, R.A., Proc. Natl. Acad. Sci. USA, 87 (1989) 2471.
43 Williams, J., Rucinski, B., Holt, J. and Niewiarowski, S., Biochim. Biophys. Acta, 1039 (1990) 81.
44 Soszka, T., Knudsen, K.A., Beviglia, L., Rossi, C., Poggi, A. and Niewiarowski, S., Exp. Cell Res., 196 (1991) 6.
45 Shebuski, R.J., Ramjit, D.R., Bencen, G.H. and Polokoff, M.A., J. Biol. Chem., 264 (1989) 21550.
46 Huang, T.-F., Holt, J.C., Kirby, E.P. and Niewiarowski, S., Biochemistry, 28 (1989) 661.
47 Savage, B., Marzec, U.M., Chao, B.H., Harker, L.A., Maraganore, J.M. and Ruggeri, Z.M., J. Biol. Chem., 265 (1990) 11766.

48 Sato, M., Sardana, M.K., Grasser, W.A., Garky, V.M., Murray, J.M. and Gould, R.J., J. Cell Biol., 111 (1990) 1713.
49 Pfaff, M., Tangemann, K., Müller, B., Gurrath, M., Müller, G., Kessler, H., Timpl, R. and Engel, J., J. Biol. Chem., 269 (1994) 20233.
50 Bartlett, P.A., Shea, G.T., Telfer, S.J. and Waterman, S., In Roberts, S.M. (Ed.) Molecular Recognition: Chemical and Biochemical Problems, The Royal Society of Chemistry, Cambridge, 1989, pp. 182–196.
51 Adler, M., Lazarus, R.A., Dennis, M.S. and Wagner, G., Science, 253 (1991) 445.
52 Saudek, V., Atkinson, R.A. and Pelton, J., Biochemistry, 30 (1991) 7369.
53 Dalvit, C., Widmer, H., Bovermann, G., Breckenridge, R. and Metternich, R., Eur. J. Biochem., 202 (1991) 315.
54 Cooke, R.M., Carter, B.G., Martin, D.M.A., Murray-Rust, P. and Weir, M.P., Eur. J. Biochem., 202 (1991) 323.
55 Dauber-Osguthorpe, P., Roberts, V.A., Osguthorpe, D.J., Wolff, J., Genest, M. and Hagler, A.T., Protein Struct. Funct. Genet., 4 (1988) 31.
56 Verlet, L., Phys. Rev., 159 (1967) 98.
57 Pfaff, M., Aumailley, M., Specks, U., Knolle, J., Zerwes, H.G. and Timpl, R., Exp. Cell Res., 206 (1993) 167.
58 Müller, G., Gurrath, M., Kessler, H. and Timpl, R., Angew. Chem., Int. Ed. Engl., 31 (1992) 326.
59 Müller, G., Gurrath, M., Kurz, M. and Kessler, H., Protein Struct. Funct. Genet., 15 (1993) 235.
60 Wistow, G., Turnell, B., Summers, L., Slingsby, C., Moss, D., Miller, L., Lindley, P. and Blundell, T., J. Mol. Biol., 107 (1983) 175.
61 Kurz, M., Mierke, D.F. and Kessler, H., Angew. Chem., Int. Ed. Engl., 31 (1992) 210.
62 Bogusky, M.J., Naylor, A.M., Pitzenberger, S.M., Nutt, R.F., Brady, S.F., Colton, C.D., Sisko, J.T., Anderson, P.S. and Veber, D.F., Int. J. Pept. Protein Res., 39 (1992) 63.
63 Peishoff, C.E., Ali, F.E., Bean, J.W., Calvo, R., D'Ambrosio, A.D., Eggleston, D.S., Hwang, S.M., Kline, T.P., Koster, P.F., Nichols, A., Powers, D., Romoff, T., Samanen, J.M., Stadel, J., Vasko, J.A. and Kopple, K.D., J. Med. Chem., 35 (1992) 3962.
64 Cotrait, M., Kreissler, M., Hoflack, J., Lehn, J.-M. and Maigret, B., J. Comput.-Aided Mol. Design, 6 (1992) 113.
65 Siahaan, T., Lark, L.R., Pierschbacher, M.D., Ruoslahti, E. and Gierasch, L.M., In Rivier, J.E. and Marshall, G.R. (Eds.) Peptides: Chemistry, Structure and Biology (Proceedings of the 11th American Peptide Symposium), ESCOM, Leiden, 1990, pp. 699–701.
66 Ruoslahti, E. and Pierschbacher, M.D., Science, 238 (1987) 491.
67 Bean, J.W., Kopple, K.D. and Peishoff, C.E., J. Am. Chem. Soc., 114 (1992) 5328.
68 Kopple, K.D., Baures, P.W., Bean, J.W., D'Ambrosio, C.A., Hughes, J.L., Peishoff, C.E. and Eggleston, D.S., J. Am. Chem. Soc., 114 (1992) 9615.
69 Gurrath, M., Ph.D. Thesis, Technische Universität München, Garching, 1992.
70 Müller, G., Ph.D. Thesis, Technische Universität München, Garching, 1992.
71 Lender, A., Yao, W., Sprengeler, P.A., Spanevello, R.A., Furst, G.T., Hirschmann, R. and Smith III, A.B., Int. J. Pept. Protein Res., 42 (1993) 509.
72 Johnson Jr., W.C., Pagano, T.G., Basson, C.T., Madri, J.A., Gooley, P. and Armitage, I.M., Biochemistry, 32 (1993) 268.
73 Barker, P.L., Bullens, S., Bunting, S., Burdick, D.J., Chan, K.S., Deisher, T., Eigenbrot, C., Gadek, T.R., Gantzos, R., Lipari, M.T., Muir, C.D., Napier, M.A., Pitti, R.M., Padua, A., Quan, C., Stanley, M., Struble, M., Tom, J.Y.K. and Brunier, J.P., J. Med. Chem., 35 (1992) 2040.
74 O'Neil, K.T., Hoess, R.H., Jackson, S.A., Ramachandran, N.S., Mousa, S.A. and DeGrado, W.F., Protein Struct. Funct. Genet., 14 (1992) 509.
75 Lam, K.S., Salmon, S.E., Hersch, E.M., Hruby, V.J., Kazmierski, W.M. and Knapp, R.J., Nature, 354 (1991) 82.
76 Houghten, R.A., Pinilla, C., Blondelle, S.E., Apple, J.R., Dooley, C.T. and Cuervo, J.H., Nature, 354 (1991) 84.
77 Scott, J.K. and Smith, G.P., Science, 249 (1990) 386.
78 Delvin, J.J., Panganiban, L.C. and Devlin, P.E., Science, 249 (1990) 404.
79 Cwirla, S.E., Peters, E.A., Barrett, R.W. and Dower, W.J., Proc. Natl. Acad. Sci. USA, 87 (1990) 6378.
80 Felici, F., Castagnoli, L., Musacchio, A., Jappelli, R. and Cesareni, G., J. Mol. Biol., 222 (1991) 301.
81 Jung, G. and Beck-Sickinger, A.G., Angew. Chem., Int. Ed. Engl., 31 (1992) 367.
82 Simon, R.J., Kania, R.S., Zuckermann, R.N., Huebner, V.D., Jewell, D.A., Banville, S., Ng, S., Wang, L., Rosenberg, S., Marlowe, C.K., Spellmeyer, D.C., Tan, R., Frankel, A.D., Santi, D.V., Cohen, F.E. and Bartlett, P.A., Proc. Natl. Acad. Sci. USA, 89 (1992) 9367.

83 Kessler, H., Angew. Chem., Int. Ed. Engl., 32 (1993) 543.
84 Holmes, M.A., Tronrud, D.E. and Matthews, B.W., Biochemistry, 22 (1983) 236.
85 Carter, D.C., Melis, K.A., O'Donnell, S.E., Burgess, B.K., Furey Jr., W.F., Wang, B.-C. and Scott, C.D., J. Mol. Biol., 184 (1985) 279.
86 Ryu, S.-E., Kwong, P.D., Truneh, A., Porter, T.G., Arthos, J., Rosenberg, M., Dai, X., Xuong, N.-H., Axel, R., Sweet, R.W. and Hendrickson, W.A., Nature, 348 (1990) 419.
87 Fujinaga, M., Delbaere, L.T.J., Brayer, G.D. and James, M.N.G., J. Mol. Biol., 184 (1985) 479.
88 Ochi, H., Hata, Y., Tanaka, N., Kakudo, M., Sakurai, T., Aihara, S. and Morita, Y., J. Mol. Biol., 166 (1983) 407.
89 Leahy, D.J., Hendrickson, W.A., Aukhil, I. and Erickson, H.P., Science, 258 (1992) 987.